Finite orbit width effect in ion collisional transport in TJ-II

J. L. Velasco, F. Castejón, and A. Tarancón

Citation: Phys. Plasmas **16**, 052303 (2009); doi: 10.1063/1.3126583
View online: http://dx.doi.org/10.1063/1.3126583
View Table of Contents: http://pop.aip.org/resource/1/PHPAEN/v16/i5
Published by the American Institute of Physics.

Finite orbit width effect in ion collisional transport in TJ-II

J. L. Velasco,[1,2] F. Castejón,[1,3] and A. Tarancón[1,2]
[1]*Instituto de Biocomputación y Física de Sistemas Complejos, 50009 Zaragoza, Spain*
[2]*Departamento de Física Teórica, Universidad de Zaragoza, 50009 Zaragoza, Spain*
[3]*Laboratorio Nacional de Fusión, Asociación Euratom/Ciemat, 28040 Madrid, Spain*

(Received 26 January 2009; accepted 9 April 2009; published online 7 May 2009)

The validity of the traditional local diffusive approach and of the use of monoenergetic calculations has been studied for the stellarator TJ-II [Alejaldre *et al.*, Fusion Technol. **17**, 131 (1990)]: it is shown to be doubtful, under some circumstances, even in a purely collisional description of transport. The diffusion in physical space starting from Dirac-delta-like initial conditions has been studied using the code Integrator of Stochastic Differential Equations for Plasmas by Castejón *et al.* [Plasma Phys. Controlled Fusion **49**, 753 (2007)]. Particles may experience large radial excursions from their original magnetic surfaces in a single collisional time. The contribution of these particles to the flux may make it nondiffusive; non-Gaussian density distributions, characterized by long tails, are observed. In the velocity space, there are important variations in the average particle kinetic energy after one collision time. We discuss the effect of this fact over the calculation of monoenergetic transport coefficients and their convolution. A simple analysis based on Hurst exponents has shown nevertheless that the description of transport by means of a pinch term and an *effective* transport coefficient is more correct than expected. © *2009 American Institute of Physics*. [DOI: 10.1063/1.3126583]

I. INTRODUCTION

Transport is usually described within the diffusion-convection paradigm (see e.g., Refs. 1 and 2). Nevertheless, this picture has its limitations and there are experimental results[3–5] that do not fit the predictions of diffusive transport models: the propagation of perturbations and long-range correlations, the scaling of the confinement time, and other transport parameters with the system size.

These phenomena led to the formulation of new models that get rid of the diffusive constraint, sometimes together with Markovianity. Some sort of nondiffusivity has been obtained by making the transport coefficients depend on quantities such as the density gradient in a nontrivial manner (see for instance Ref. 6). Recently, a unified framework for transport models is starting to be developed based on fractional derivative operators and continuous time random walks, see Refs. 7–9 and references therein. In some cases, these models obtained quantitative agreement with turbulence transport calculations, see, e.g., Ref. 8. A battery of numerical techniques (see, e.g., Refs. 10–12) has been developed for these studies, and some of them will be employed in this work.

Nevertheless, the Fokker–Planck equation that underlies neoclassical transport calculations can still be relevant for describing nondiffusive transport features (see Refs. 13 and 14 and references therein): "Fickian" transport derives from the Fokker–Planck equation only for the one-dimensional case. Indeed, nondiffusive effects can be observed in kinetic calculations due to a competence between the characteristic time and space scales. In particular, the effect that the ion trajectories (and specially their large radial excursions) have on the collisional transport has been studied for different devices.[15–18] In the stellarator TJ-II,[19] it was investigated in a low density electron cyclotron heating (ECH) plasma, in the frame of a global study of kinetic transport in the absence of the customary assumptions of neoclassical models.[20] Other calculations[21] have shown (although some of the standard neoclassical assumptions remained) that the diffusive approach is valid for the stellarator Wendelstein 7-X,[22] but not for TJ-II.

In this work, a deeper insight is sought for three types of TJ-II plasmas: an ECH low-collisionality plasma, an intermediate regime created by means of simultaneous ECH and neutral beam injection (NBI) heating, and a high-collisionality NBI plasma. The study is performed in different radial positions of the plasma, since it is possible to have kinetic transport of different natures at different regions, see, e.g., Refs. 20 and 23. In our simulated plasmas presented in Sec. III, the collision time does not have strong radial dependency, since in our region of interest (ρ between 0.1 and 0.7) the density and ion temperature profiles are rather flat. Here, $\rho \equiv \sqrt{\psi/\psi_0}$ is the normalized radial coordinate and ψ and ψ_0 are the magnetic fluxes through the local and the last closed magnetic surfaces. Nevertheless, the magnetic structure is different and so is the experimentally observed radial electric field. Extremely collisional plasmas have been also considered in order to explore the limit in which transport should be diffusive and the neoclassical approximations should apply.

For the three plasmas considered, we study the effect of the radial electric field, which is taken from the experiment, on the particle orbits: their average radial movement (whose velocity is the *pinch*) and the size of their radial excursions. We then make a discussion on the validity of the local ansatz and the use of monoenergetic calculations.[24] Finally, we obtain a rough estimate of the Hurst exponent of the system. These are standard tools used to study general transport phenomena such as anomalous plasma transport.[10–12]

The reminder of this paper is organized as follows. Section II discusses the domain of validity of the local ansatz for TJ-II. Section III describes the plasma profiles considered and the calculation method. Section IV describes the results [probability density function (PDF), pinches, and Hurst exponents] for the three plasmas. The conclusions come in Sec. V.

II. THE DOMAIN OF VALIDITY OF THE LOCAL ANSATZ AND THE MONOENERGETIC CALCULATIONS

Neoclassical transport studies[24] attempt to determine the transport coefficients that relate the fluxes to the thermodynamical forces. This implies assuming that transport is diffusive and therefore the particle and heat radial fluxes can be written[21,24,25] as

$$\Gamma_s = -D_1^s n_s \left(\frac{1}{n_s}\frac{dn_s}{d\rho} - \frac{Z_s e}{T_s}\frac{d\Phi}{d\rho} + \left(\frac{D_2^s}{D_1^s} - \frac{2}{3}\right)\frac{1}{T_s}\frac{dT_s}{d\rho} \right), \quad (1)$$

$$q_s = -D_2^s n_s T_s \left(\frac{1}{n_s}\frac{dn_s}{d\rho} - \frac{Z_s e}{T_s}\frac{d\Phi}{d\rho} + \left(\frac{D_3^s}{D_2^s} - \frac{2}{3}\right)\frac{1}{T_s}\frac{dT_s}{d\rho} \right). \quad (2)$$

These coefficients D_1^s, D_2^s, and D_3^s (corresponding to species s) are local, i.e., they depend only on the density n_s, temperature T_s, and radial electric field $d\Phi/d\rho$ at a given radial position ρ. For this to be true, the local ansatz must be fulfilled: the radial orbits of the particles must be narrow enough so that the transport properties depend only on the characteristics of the local magnetic surface. If this happens, the system is assumed to be near the equilibrium and its distribution function close enough to the Maxwellian. Then, the transport coefficients are usually calculated by convolution of monoenergetic coefficients with the local Maxwellian,[24]

$$D_j^s = \frac{2}{\sqrt{\pi}} \int_0^\infty dx_s x_s^{(2j-1)/2} D(x_s) e^{-x_s}, \quad (3)$$

where $x_s = m_s v^2 / kT_s$ is the normalized kinetic energy. This procedure has been shown to be equivalent to the calculation of transport coefficients by including energy scattering,[24] i.e., by taking into account the dispersion both in spatial and velocity coordinates.

Nevertheless, estimating the monoenergetic coefficients implies calculating the diffusion of particles of fixed kinetic energy. One therefore neglects the effect of energy scattering due to particle collisions and the change in the kinetic energy due to the radial drift in the presence of a radial electric field. The former assumption is quite reasonable as long as the real particle distribution does not separate too much from the Maxwellian, since the convolution is expected to account for the effect of energy thermalization. This fact is not independent of the local ansatz; its domain of validity is the same. However the effect of the electric field may be important in case of large radial drifts and/or strong fields.

Therefore, as it has been widely discussed (see, e.g., Refs. 21 and 24), the above approximation has a domain of validity determined by the relation between the strength of the electric field and the kinetic energy:

- The electric field must be strong enough so that it reduces the $\vec{\nabla}B$ drift of the ripple-trapped particles. A threshold is usually defined:[26,27] For fields such that $Ze\Phi/kT > 2a/R$, i.e., such that the ratio between the potential and the kinetic energy is higher than the inverse aspect ratio, the ripple regime is considered to be suppressed.[26]
- The work done by the electric field over the drifting particles must be low enough compared to their kinetic energy, so that the kinetic energy is an *approximately* conserved quantity. This upper threshold, although recognized,[21,25] is not usually quantified. A straightforward definition would be $eE\Delta\rho/kT < 1$, although one should keep in mind that the radial size of the orbits $\Delta\rho$ depends on $\vec{E}$.[26]

The diffusive approach works within these two limits. Nevertheless, we find that both conditions cannot be fulfilled at the same time in low collisionality plasmas of TJ-II:

- The local ansatz does not hold for the long-mean-free-path regime, as it has been already claimed in a perturbative computation of the distribution function[21] and in recent calculations.[20,28] Thus it seems that, although $Ze\Phi/kT = 2a/R$ is fulfilled, this limit, calculated for an $l=2$ stellarator, is not valid for TJ-II, whose magnetic field structure is much more complex.
- The potential profiles in typical ECH plasmas (see Fig. 1 below) may vary several hundreds of volts from the center to the edge. Therefore, even small radial excursions imply important variations in the kinetic energy.

In this work, we study these two related effects: wide radial excursions in the presence a large electric field and lack of kinetic energy conservation. With this in mind, we calculate the guiding-center trajectories of a large number of ions starting at fixed radial positions with a Maxwellian velocity distribution. We measure the PDF of the radial displacements of ions; this function is composed of a convective term (pinch) and a dispersion term, and both are estimated. The former is clearly non-negligible for plasmas of low collisionality, hence the kinetic energy is not conserved, which casts doubts over the monoenergetic approach. For the same plasmas, we obtain non-Gaussian radial distributions, characterized by long tails; this shows inappropriate the diffusive treatment.[26,27]

III. THE CALCULATION METHOD AND THE PLASMA REGIMES

We perform these calculations by means of the Integrator of Stochastic Differential Equations for Plasmas (ISDEP) code.[20] We calculate the reduced distribution function (RDF) of test ions in the guiding-center approximation, in the presence of an electrostatic field, and considering collisions with a background composed of electrons and ions (each of them distributed according to a Maxwellian). We solve the

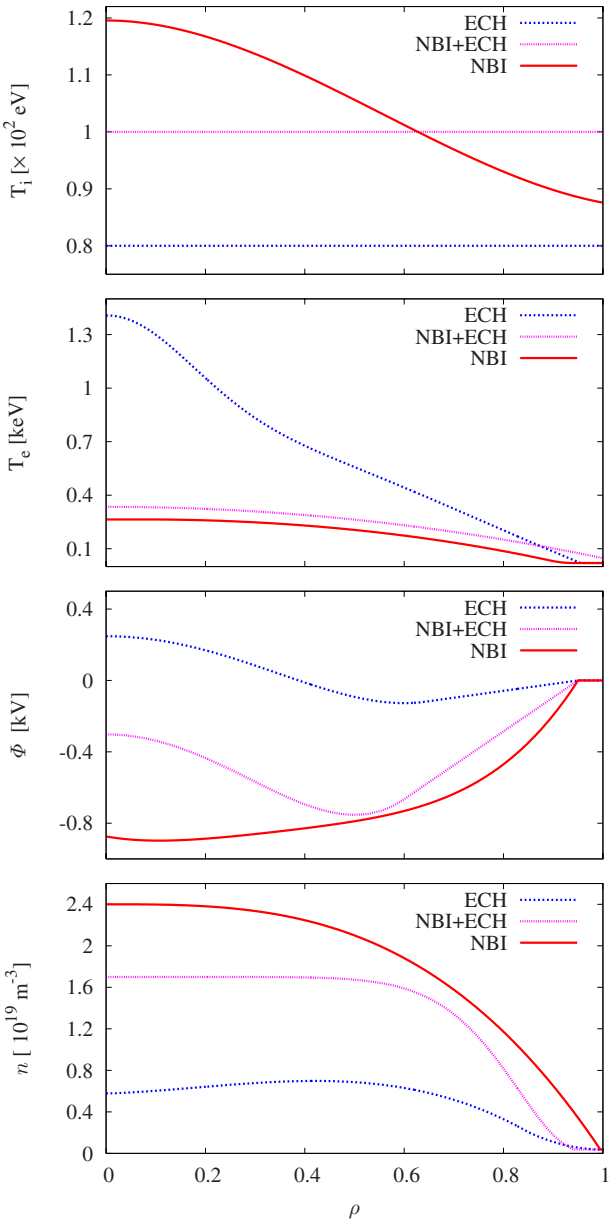

FIG. 1. (Color online) Plasma radial profiles of the three regimes.

Fokker–Planck equation describing the evolution of the RDF by means of a set of Langevin equations. This allows us to avoid additional assumptions such as small radial excursions, energy conservation, or local transport. This is obviously crucial in our study. Furthermore, it allows for its use in the volunteer-computing platform Zivis,[29] where huge statistics is obtained and therefore great accuracy is achieved.

Concretely, we calculate the guiding-center trajectories of a large number of ions starting at a fixed value of the radial position ρ (randomly distributed along the toroidal and poloidal coordinates) with a Maxwellian velocity distribution and we measure the PDF of the radial displacements of ions.

We undertake this calculation for three different regimes in TJ-II: ECH, NBI, and ECH+NBI. The temperature, density, and electrostatic potential profiles are taken similar to those experimentally measured. The density and the electron temperature are obtained from Thomson-scattering measurements,[30] the ion temperature profiles are taken from the charge exchange neutral particle analyzer diagnostic,[31] in shot to shot experiments. Finally, the electrostatic potential comes from heavy ion beam probe measurements.[32] The NBI and the ECH plasmas have already been numerically studied in Refs. 33 and 34.

In Fig. 1, we show a low density, low collisional ECH plasma. The core plasma is in electron root confinement regime.[35] Hence the electric field is positive in this region and the electron temperature profile is peaked. That of the ion temperature is almost flat within the error bars. This fact was found in Ref. 36 and we in fact attribute it[33] to the existence of a nondiffusive heat ion transport. The density profile is hollow due to the ECH-induced pump out (see, e.g., Refs. 37 and 38). The electrostatic potential is nonmonotonic due to a transition from the electron root (positive electric field) in the center of the device to the ion root (negative electric field) in the edge.

We also consider a NBI plasma. The density is high and the electron temperature is low, with parabolic profiles, as in Ref. 39. In this case, the ion temperature is not flat, but presents a steeper gradient. The potential corresponds to a plasma that is in the ion root along the whole range in the minor radius: it is monotonic (except in a small region close to the center) and negative.

The intermediate regime has similar profiles to the ECH case, with ion and electron temperatures slightly higher. The density is also higher than in the ECH case. The electrostatic profile presents also a minimum near $\rho=0.5$, as in the ECH plasma, but the electric field is higher.

The collision time ranks from $\sim 7\times 10^{-5}$ s in the NBI plasma and $\sim 8\times 10^{-5}$ s in the ECH+NBI plasma to $\sim 2\times 10^{-4}$ s of the ECH plasma. The rest of the time scales can be considered to be the same for the present calculations: the period of the oscillatory motion of a trapped particle in a banana orbit ($\sim 10^{-5}$ s), the time needed to complete a cycle around TJ-II ($\sim 10^{-4}$ s), and the time needed for the ions to react to changes in the electric field ($\sim 5\times 10^{-3}$ s). There is also the particle confinement time of particles: it is of the order of ~ 0.01 s, but it highly depends on the conditions of the simulation, mainly the initial radial position, but also on the electric field and the collisionality.

The three-dimensional (3D) magnetic configuration is included in the simulation by using a mesh that fits the magnetic surfaces in real space. We made a study on the convergence of the algorithm used, developed by Kloeden and Pearson. We found that a time step $\Delta t=2\times 10^{-8}$ s is small enough for our calculation (see Ref. 20 for details).

IV. RESULTS

A. Pinch analysis

We are interested in the variation in the radial electrostatic potential along the particle trajectories in order to check the local ansatz and the validity of the monoenergetic approach. We want therefore to separate the *pinch effect* from the energy, i.e., the variation in the kinetic energy caused only by the radial displacement of the ions, from the thermalization effect (remember that we are using a collision

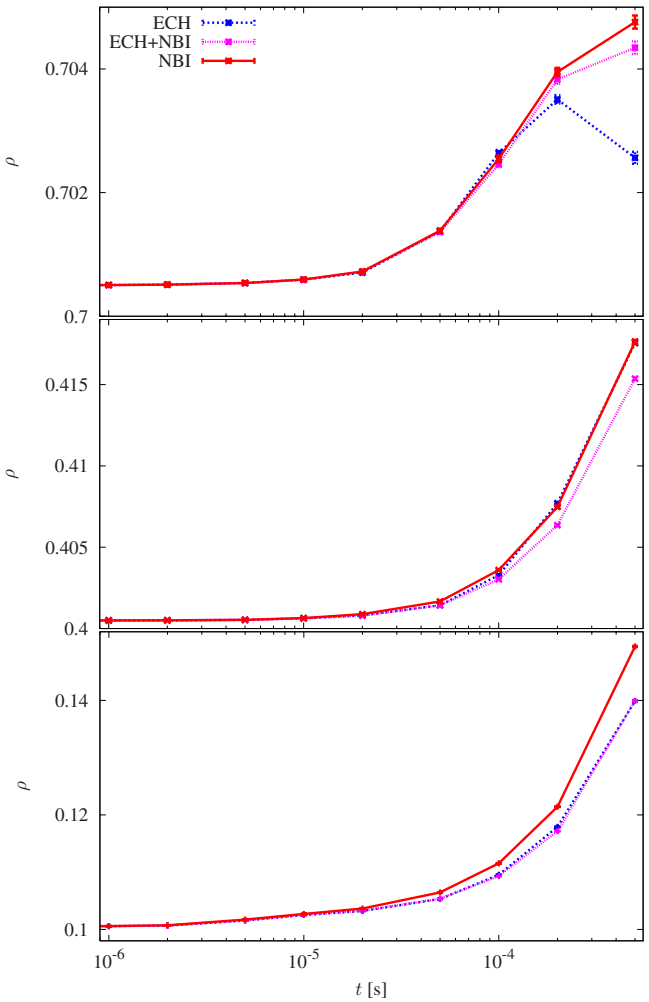

FIG. 2. (Color online) Average radial coordinate ρ of the ions as a function of time without electric field for the three regimes described in Sec. III and for the three starting radial positions.

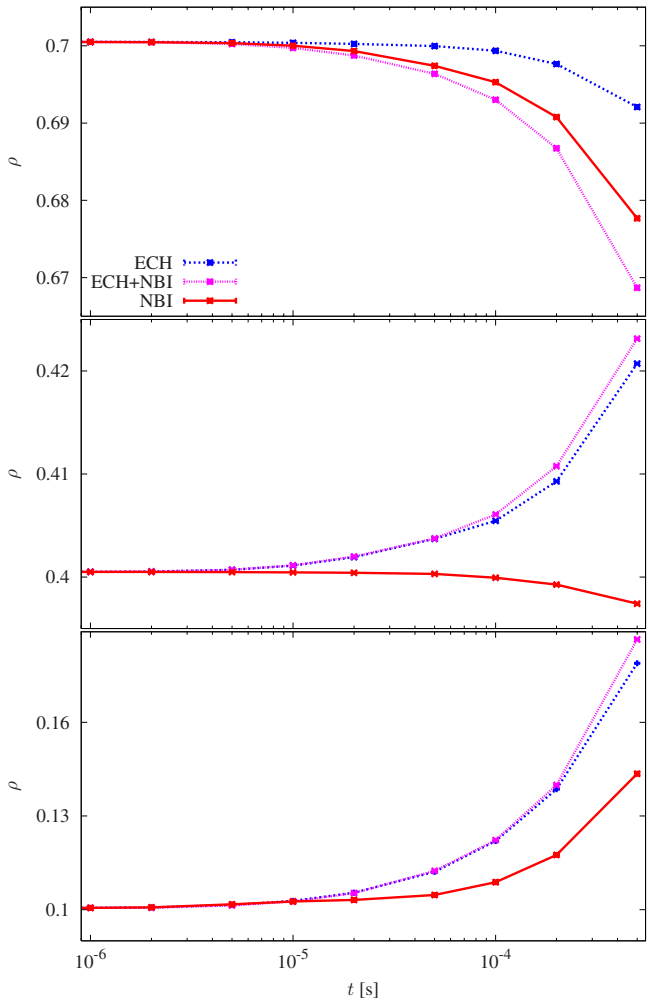

FIG. 3. (Color online) Average radial coordinate ρ of the ions as a function of time, with the experimental electric field included in the calculations.

operator with energy scattering). We thus calculate the evolution of the average radial coordinate of the ions. The action of the potential on the kinetic energy is then quantified as $\Delta\Phi(t) \equiv \Phi[\langle\rho\rangle(t)] - \Phi[\langle\rho\rangle(0)]$. These data, obtained from the calculations with ISDEP described in Sec. III, have been summarized in Figs. 2 and 3 and in Table I.

In Fig. 2 we show the time evolution, up to two collision times (see the previous section), of the average radial coordinate of the ions. We present in different panels the data for ions starting at $\rho=0.1$, 0.4, and 0.7. This time limit has been set according to the common practice of Monte Carlo codes, consisting in following monoenergetic test particles for several collision times. In this simulation, no radial electric field is considered. Although the electric field of Fig. 1 is actually experimentally observed in TJ-II, this exercise enables us to compare the balance between the magnetic structure and the collisions. One can see that the pinch evolves similarly in the three plasmas for times of the order of $t \approx 10^{-5}$ s. The points start to separate only at the collisional time scale; at shorter times, the magnetic structure (the same in the three cases) drives the pinch. The difference between the density gradients near the edge must be in the origin of the differences for the late times at $\rho=0.7$.

More information can be gathered from Fig. 3, where we repeat the calculation of Fig. 2 but including the experimental electric field. The qualitative differences between the three potentials reflect in the data: besides reducing the orbit size, the electric field acts as a thermodynamical force, driving the ions toward the minimum of the potential. In the case of ions with initial position $\rho=0.7$ (and also $\rho=0.4$ for the

TABLE I. Average variation in the radial electrostatic potential along the orbit for different plasma regimes and starting radial positions.

Plasma	$\rho(t=0)$	$\Delta\Phi(t_{col})$ (V)	$\Delta\Phi(2t_{col})$ (V)
ECH	0.1	20	50
ECH	0.4	10	20
ECH	0.7	1.5	3
ECH+NBI	0.1	15	35
ECH+NBI	0.4	5	10
ECH+NBI	0.7	10	25
NBI	0.1	<1	<1
NBI	0.4	<1	<1
NBI	0.7	<1	<1

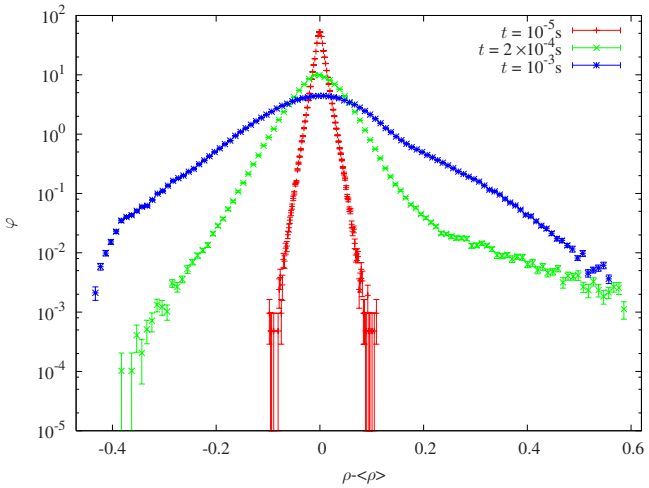

FIG. 4. (Color online) PDF of the radial displacements for the ECH plasma at three different times. The starting position is $\rho=0.4$.

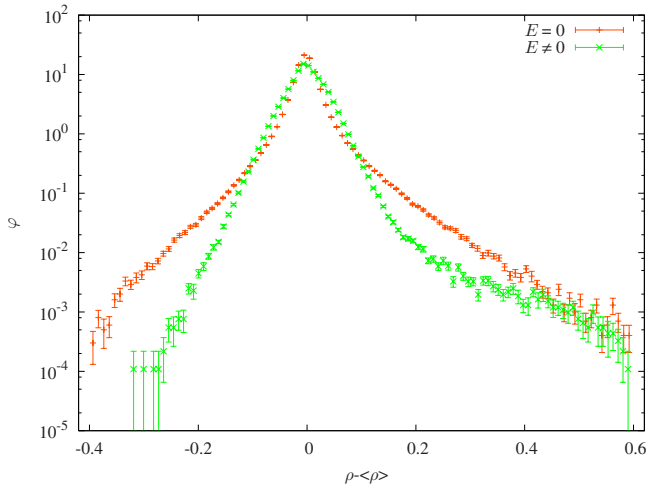

FIG. 5. (Color online) Comparison of the PDFs with and without electric field at $\rho=0.4$ for the ECH plasma.

NBI plasma), this effect overcomes *on average* the outward drift due to the magnetic ripple and thus improves the confinement. We show in the following section that this happens in the same time scale that the electric fields acts on the orbit width.

Table I shows that, for the ECH plasma, the variation in the potential along the orbit in two collision times is about one-half of the kinetic energy. In these conditions, the monoenergetic approach is quite doubtful if the so-calculated monoenergetic coefficient has a sharp variation with the collisionality ν^*, since the latter depends in turn on the kinetic energy ($\nu^* \propto 1/v^3$). This would lead to wrong results obtained in the convolution. This effect is very strong in sensitive calculations such as that of the bootstrap current, see, e.g., Fig. 7 in Ref. 25. There, a variation of the order of 50% in the kinetic energy (i.e., $\approx$75% in ν^*) around $\nu^*=0.05$ (like in TJ-II outer regions) leads to a variation of about 100% in the calculated coefficient. This may also affect the calculation of other coefficients.[25,27]

A similar result is obtained for the intermediate regime. For the NBI plasma, the variation is negligible, and therefore, regarding this extent, the monoenergetic calculation works properly.

B. The PDF of radial displacements

In Fig. 4 we show the PDF for the ECH plasma (taking into consideration the experimental electric field in the calculations), with starting position $\rho=0.4$, for several selected times. The abscissa scale has been shifted by $\langle\rho\rangle$. One can see that at a time $t=10^{-5}$ s, quite lower than the collision time, the PDF is nearly Gaussian. This is a consequence of the initial distribution of velocities, which is Maxwellian, since the selected time is shorter than all the relevant characteristic time scales discussed. For a time of the order of the collision time, a long tail develops. Since ρ takes values between 0 and 1, Fig. 4 shows that, in a single collision time, there are particles that arrive at the edge of the plasma (the ones located at $\rho=-\langle\rho\rangle=0.6$). The asymmetry in the PDF should be attributed to the asymmetry in the electrostatic potential profile around the birth point of the particles, see Fig. 1.

In order to check the effects of the electrostatic potential profile, the same calculation has been performed with zero electric field and the results are plotted in Fig. 5 for the time $t=5\times10^{-4}$ s. One can see that the electric field acts by reducing the orbit width, as expected. It is also clear that, although the characteristic time scale for the electric field acting on $\langle\rho\rangle$ is $\sim5\times10^{-3}$ s,[20] its effects on the PDF appear at shorter times, comparable with the collision time. As a consequence of this, the asymmetry in the PDF stays for several collision times; in Fig. 4, for $t=5\times10^{-4}$ s, the PDF is clearly non-Gaussian.

The non-Gaussianity is more pronounced in the case without electric field. The effect of the field, not present in this last calculation, is to reduce the orbit size and hence to prevent the ions from exploring the complex magnetic structure of TJ-II.

The NBI plasma, on the contrary, shows a nearly Gaussian PDF at a time of the order of the collision time, see Fig. 6. On the one hand, this effect can be understood once more in terms of competence between effects: for this high-collisionality plasma, the collision time is lower than the rest of characteristic times. Therefore, this effect is the prevalent mechanism in the evolution of the PDF. On the other hand, the electric field is low in the region around $\rho=0.4$ and negative in all the ρ range, so that it does not change the shape of the PDF, since the $\vec{E}\times\vec{B}$ term results into a global drift.

An intermediate situation is found in Fig. 7 for the ECH+NBI plasma. Here, the collisionality is higher than in the ECH case and the potential well is more symmetric. The combined action of both effects avoids the formation of a tail such as that of the ECH case. Nevertheless, the PDF is asymmetric and the tails extend almost to the edge of the plasma in a few collision times. A flattening of the PDF is observed for intermediate times, near the minimum of the electrostatic

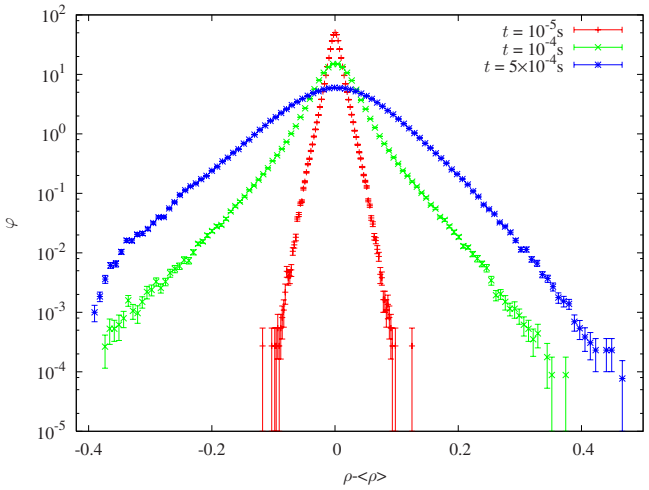

FIG. 6. (Color online) PDF of the radial displacements for the NBI plasma at three different times. The starting position is $\rho=0.4$.

potential structure. This is a zone of relatively enhanced transport, occurring where the electric field is minimum and cannot reduce the ripple transport.

For the sake of completitude, we also simulated a rather artificial case of extremely high collisionality. The collision time was set to be the lowest time scale in the problem. As a consequence of this, the obtained PDF was Gaussian.

C. Estimation of Hurst exponents

The Hurst exponent H is utilized in plasma physics in order to study the propagation of pulses or inhomogeneities in complex systems that present stochastic features (see, e.g., Refs. 40 and 41 and references therein). This is the case of ion transport in magnetic fusion devices, due to the interaction processes between particles: binary collisions and the fluctuation of the electric and magnetic fields (the latter not considered in this paper).

In many cases, the nature of the microscopic movement of the particles is assumed to be that of the well known Brownian random walks.[42,43] The *steps* have well-defined characteristic lengths and times. In one dimension, one would write

$$\rho(t) = \rho_0 + \int_0^t \mathrm{d}t'\,\xi(t'), \tag{4}$$

where $\xi(t)$ is a Gaussian uncorrelated noise. The result is a Fick-type law[44] for the fluxes, which are then proportional to the gradients. The system modeled with this equation exhibits diffusive behavior,

$$\langle(\rho-\rho_0)^2\rangle \propto t. \tag{5}$$

Nevertheless, many interesting processes such as transport by turbulent flows, exhibit anomalous diffusion,[3–5]

$$\langle(\rho-\rho_0)^2\rangle \propto t^{2H}, \quad H \neq 0.5. \tag{6}$$

Here, $H>0.5$ corresponds to superdiffusive behavior ($H=1$ is called ballistic) and $H<0.5$ to subdiffusion. The lack of defined characteristic lengths in the system and to the presence of time correlations has been proposed as the key factor.[45–47] Hence, the exponent H can be employed as a measurement of these correlations in the microscopic scale of the system: superdiffusive/diffusive/subdiffusive transport, see Eq. (6), implies correlated/uncorrelated/anticorrelated increments in the movement $\rho(t)\rightarrow\rho(t+\mathrm{d}t)$.

From the discussion above, it is clear that in a purely local and Markovian system, one would expect a value of $H=0.5$, corresponding to diffusive behavior and Gaussian PDFs. The Brownian random walk would not be able to model nondiffusive behavior, since the noise in Eq. (4) is uncorrelated (and a generalization would the be required, such as continuous time random walk). This would seem to be the case for the solution of a Fokker–Planck equation, since it is equivalent to a set of Itô stochastic differential equations describing a Markovian process. Nevertheless, Eq. (4) is one dimensional. Apart from the Itô diffusion in the velocity space, there is in our case a deterministic evolution in a complex magnetic geometry. As a consequence of this fact, transport is usually modeled as a pinch term plus a diffusion term. This description could not be valid in principle for the low collisionality regime of TJ-II plasmas, where we obtained non-Gaussian PDFs in our calculations. Hence, we claim to be able of obtaining nondiffusive behavior without the need of resorting to more complex models: it is enough the action of collisions in the presence of an strong electric field and a magnetic configuration of enough complexity and large ripple.

The precise calculation of the Hurst exponent is a difficult task, which usually involves a very sensitive study of the tails of the distribution functions and therefore a huge amount of statistics.[40,41] Thus we do not intend here but to obtain rough estimations of the possible nondiffusive character of the collisional transport, in order to complete the above discussion.

In the previous section, we calculated the distribution of radial particle displacements. If the parameter H is well defined, the second moment of this distribution $\Delta\rho\equiv\langle(\rho-\langle\rho\rangle)^2\rangle^{1/2}$ will behave as $\Delta\rho\propto t^H$. Since we do not include a source, the number of particles will decrease monotonically:

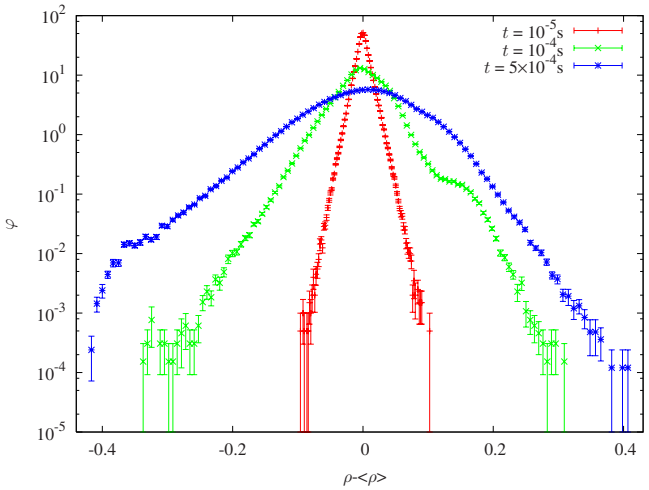

FIG. 7. (Color online) PDF of the radial displacements for the ECH+NBI plasma at three different times. The starting position is $\rho=0.4$.

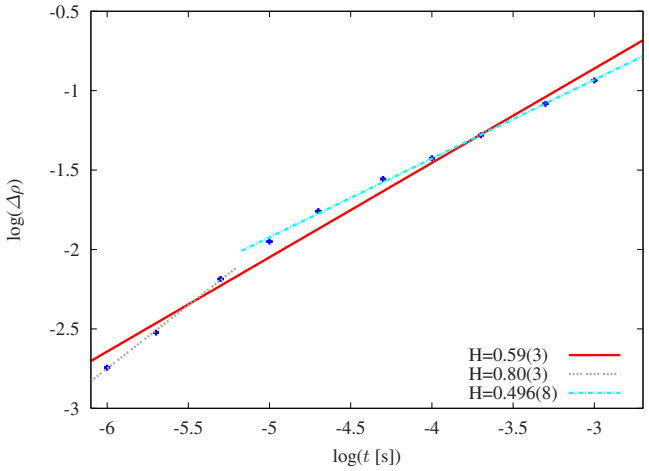

FIG. 8. (Color online) Log-log plot of the second moment of the PDF vs the time for the ECH plasma at $\rho=0.4$. The Hurst exponent is extracted for two different time scales.

particles are lost in the edge, $\rho=1$. In the following, we include data for times at which at least 95% of the particles remain. This is a rather arbitrary choice, but our results are not very sensitive to it.

Our data usually seem to fit $\Delta\rho \propto t^H$ in two different regimes. Including in the analysis times $t<10^{-5}$, lower than the collision time, the behavior is nearly ballistic. Employing longer times, the calculated H decreases, due to collisions. This is consequence of the competence between time scales in our simulated plasmas and can be tracked in the experiments: the superdiffusive behavior may be observed experimentally when the time scale of the considered phenomenon is fast enough. Figure 8 shows the fit for the ECH plasma particles with birth position at $\rho=0.4$. The electric field is included in the simulations. The existence of two different regimes of H can be clearly observed.

In Fig. 9, we summarize the data by sketching H radial profiles. As we have discussed, measuring H is a very complex task and we here only discuss qualitative trends. For the points with continuous lines, we compute the trajectories up to $t=10^{-5}$ s, for the points with dashed lines, up to $t=2\times10^{-3}$ s, which means several collision times.

In all cases, for short times, the behavior of the PDFs seems to be fully determined by the magnetic configuration. This is in agreement with our previous discussion on time scales. We observe a sharp transition between $\rho=0.1$ and outer radii, which we interpret to be caused by the variation in the ripple, which grows roughly with ρ^2. According to these results, it seems that the ripple transport is naturally suppressed for inner radii, while, in the outer radii, it is only suppressed when a radial electric profile appears. In fact, we observed slight subdiffusion at this position in all the simulated plasmas.

The effect of the electric field is to approach the system to diffusive behavior. This is done by reducing the ripple transport and hence reducing the orbits widths. This has been analyzed in detail in the previous sections.

No great difference is observed between the three regimes, which is quite surprising according to our previous

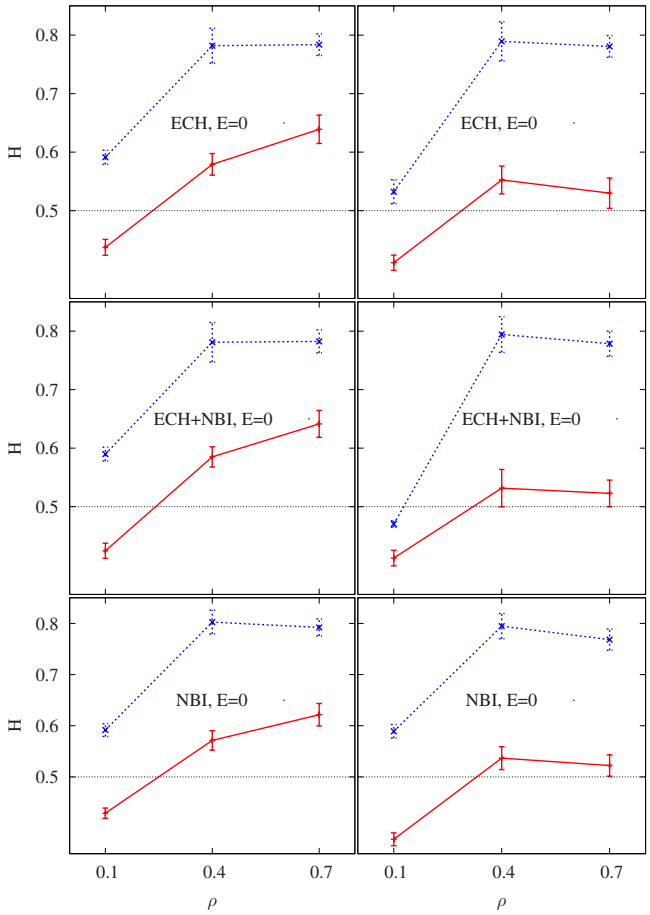

FIG. 9. (Color online) Radial profile of the Hurst exponent for all the plasmas simulated with (continuous) data up to $t=10^{-5}$ s and (dashed) up to $t=2\times10^{-3}$ s.

discussion and to the results shown in previous studies[20] for low collisionality plasmas. The conclusion is that our rough calculation of H, by means of $\Delta\rho$ is not very precise, and hides the fact that there exist long tails in the distribution for these plasmas. On the other hand, the results shown in Fig. 9 allow for the definition of *effective* transport coefficients in diffusive models $D_{\text{eff}} \equiv |\Gamma/\nabla n|$. According to our results in Sec. IV A, these coefficients could not be monoenergetic and a pinch term must also be included. The pinch and the *effective diffusion* would therefore roughly include the effect of the orbits width, but the PDF tails would be underestimated. Since these particles are usually in the energetic tail of the Maxwellian, this would underestimate the heat transport: The nondiffusive features are more pronounced than in particle transport.

V. CONCLUSIONS

The PDF of the radial displacements of ions is calculated for several TJ-II plasmas of different collisionalities and electric fields. We make so by launching a large number of ions at selected radial positions according to a Maxwellian distribution in the velocity space. By using ISDEP code, the 3D magnetic configuration, the radial electric field, and the collisions with the background are taken into account. This calculation procedure is mandatory since the kinetic energy

is not conserved in the presence of strong electric field and in conditions of wide radial excursions. This has been shown *a posteriori* in our calculations and it invalidates the monoenergetic approach. In this way, we also consider the dispersion in the velocity space from the beginning.

For all the plasmas simulated here, there are ions that perform wide radial excursions in a single collision time, therefore not fulfilling the local ansatz. This means that there exists a non-negligible particle population that will present nonlocal transport features. For low-collisionality plasmas, the measured PDF is non-Gaussian, with a clear asymmetry caused by the electric field; in this regime, the kinetic transport is not diffusive.

A rough estimate of the Hurst exponent profiles has been obtained for different time scales for the three plasmas. We interpret that, in the time scale driven by the magnetic ripple, transport is more ballistic for outer radii. In the long time scale, we observe that, as expected, the diffusive character is enhanced by the electric field. Thus, a study of perturbative phenomena may yield different qualitative results, i.e., transport of different nature (diffusive or nondiffusive), depending on the time scale considered.

Hurst exponents not far from 0.5 are obtained, showing that the description of ion transport by means of a pinch term and an effective diffusion coefficient is not so far from reality. Nevertheless, the long PDF tails, composed of energetic particles, would be ignored in this way. Therefore, some kinetic effects that can appear in the experiment cannot be explained by such model. This type of effects will be more important in heat transport, where the effect of fast particles is more relevant.

It is clear from our discussion that the full width of the ion orbits is to be accounted for in the calculation of transport. Further analyses are being carried out in order to extract systematic behavior of the PDF and to study the impact that these findings have in the description of the heat and particle fluxes.

ACKNOWLEDGMENTS

The authors are grateful to Iván Calvo for discussions. They also acknowledge partial financial support from the European Commission through Contract Nos. EGEE-II-031688 and int.eu.grid 03185. J.L.V. is a DGA (Aragón, Spain) fellow. The calculations presented in this work have been performed using the computing platform ZIVIS. The authors are indebted to the participants in this project and to the Zaragoza Council (Spain).

[1] F. L. Hinton and R. D. Hazeltine, Rev. Mod. Phys. **48**, 239 (1976).
[2] S. P. Hirshman and D. J. Sigmar, Nucl. Fusion **21**, 1079 (1981).
[3] D. del-Castillo-Negrete, B. A. Carreras, and V. E. Lynch, Phys. Plasmas **11**, 3854 (2004).
[4] B. A. Carreras, IEEE Trans. Plasma Sci. **25**, 1281 (1997).
[5] K. W. Gentle, R. V. Braveneck, G. Cima, H. Gasquet, G. A. Hallock, P. E. Phillips, D. W. Ross, W. L. Rowan, and A. J. Wootton, Phys. Plasmas **2**, 2292 (1995).
[6] F. Ryter, Y. Camenen, J. C. DeBoo, F. Imbeaux, P. Mantica, G. Regnoli, C. Sozzi, U. Stroth, ASDEX Upgrade Team, DIII-D Team, FTU Team, JET-EFDA Contributors, TCV Team, Tore Supra Team, and W7-AS Team, Plasma Phys. Controlled Fusion **48**, B453 (2006).
[7] R. Balescu, *Aspects of Anomalous Transport in Plasmas* (Institute of Physics Publishing, Bristol, 2005).
[8] D. del-Castillo-Negrete, Phys. Plasmas **13**, 082308 (2006).
[9] E. W. Montroll and G. Weiss, J. Math. Phys. **6**, 167 (1965).
[10] R. Sánchez, B. A. Carreras, D. Newman, V. Lynch, and B. Ph. van Milligen, Phys. Rev. E **74**, 016305 (2006).
[11] M. Gilmore, C. Yu, T. Rhodes, and W. Peebles, Phys. Plasmas **9**, 1312 (2002).
[12] B. A. Carreras, B. Ph. van Milligen, M. A. Pedrosa, R. Balbín, C. Hidalgo, D. E. Newman, E. Sánchez, M. Frances, I. García-Cortés, J. Bleuel, M. Endler, S. Davies, and G. F. Matthews, Phys. Rev. Lett. **80**, 4438 (1998).
[13] D. F. Escande and F. Sattin, Phys. Rev. Lett. **99**, 185005 (2007).
[14] D. F. Escande and F. Sattin, Phys. Plasma Phys. Controlled Fusion **50**, 1 (2008).
[15] A. Ejiri and Y. Takase, Nucl. Fusion **47**, 403 (2007).
[16] J. P. Christiansen and J. W. Connor, Plasma Phys. Controlled Fusion **48**, 1551 (2006).
[17] T. Kurki-Suonio, J. A. Heikkinen, and S. I. Lashkul, Phys. Plasmas **14**, 072510 (2007).
[18] W. X. Wang, G. Rewoldt, W. M. Tang, F. L. Hinton, J. Manickam, L. E. Zakharov, R. B. White, and S. Kaye, Phys. Plasmas **13**, 082501 (2006).
[19] C. Alejaldre, J. J. Alonso, J. Botija, F. Castejón, J. R. Diaz, J. Guasp, A. López-Fraguas, L. García, V. I. Krivenski, R. Martin, A. P. Navarro, A. Perea, A. Rodríguez-Yunta, M. Sorolla, and A. Varias, Fusion Technol. **17**, 131 (1990).
[20] F. Castejón, L. A. Fernández, J. Guasp, V. Martin-Mayor, A. Tarancón, and J. L. Velasco, Plasma Phys. Controlled Fusion **49**, 753 (2007).
[21] V. Tribaldos and J. Guasp, Plasma Phys. Controlled Fusion **47**, 545 (2005).
[22] M. Wanner and W7-X Team, Plasma Phys. Controlled Fusion **42**, 1179 (2000).
[23] V. I. Vargas, D. López-Bruna, J. Guasp, J. Herranz, T. Estrada, F. Medina, M. A. Ochando, J. L. Velasco, J. M. Reynolds, J. A. Ferreira, D. Tafalla, F. Castejón, A. Salas, and TJ-II Team, Ciemat Technical Report, No. 1162, 2009.
[24] W. Lotz and I. Nürenberg, Phys. Fluids **31**, 2984 (1988).
[25] K. Allmaier, S. V. Kasilov, W. Kernbichler, and G. O. Leitold, Phys. Plasmas **15**, 072512 (2008).
[26] W. Lotz, J. Nurenberg, and A. Schluter, J. Comput. Phys. **73**, 73 (1987).
[27] V. Tribaldos, Phys. Plasmas **8**, 1229 (2001).
[28] F. Castejón, J. M. Reynolds, J. M. Fontdecaba, R. Balbín, J. Guasp, D. López-Bruna, I. Campos, L. A. Fernández, D. Fernández-Fraile, V. Martín-Mayor, and A. Tarancón, Fusion Sci. Technol. **50**, 412 (2006).
[29] B. Antolí, F. Castejón, A. Giner, G. Losilla, J. M. Reynolds, A. Rivero, S. Sangiao, F. Serrano, A. Tarancón, R. Vallés, and J. L. Velasco, CEDI: II Congreso Español de Informática, Jornadas de Paralelismo, Zaragoza, Thomson Editores, España, 2007, p. 523.
[30] J. Herranz, I. Pastor, F. Castejón, E. de la Luna, I. García-Cortés, C. J. Barth, E. Ascasíbar, J. Sánchez, and V. Tribaldos, Phys. Rev. Lett. **85**, 4715 (2000).
[31] R. Balbín, S. F. L. Tabarés, V. Tribaldos, S. Petrov, and TJ-II Team, *Proceedings of the 30th EPS Conference on Controlled Fusion and Plasma Physics*, St. Petersburg, Russia, 2003 (European Physical Society, Mulhouse, 2003) Vol. 27A, p. 1.23.
[32] A. V. Melnikov, C. Hidalgo, A. A. Chmyga, N. B. Dreval, L. G. Eliseev, S. M. Khrebtov, A. D. Komarov, A. S. Kozachok, L. I. Krupnik, I. Pastor, M. A. Pedrosa, S. V. Perfilov, K. McCarthy, M. A. Ochando, G. Van Oost, C. Silva, B. Goncalves, Yu. N. Dnestrovskij, S. E. Lysenko, M. V. Ufimtsev, and V. I. Tereshin, Fusion Sci. Technol. **46**, 299 (2004).
[33] J. L. Velasco, F. Castejón, L. A. Fernández, V. Martin-Mayor, A. Tarancón, and T. Estrada, Nucl. Fusion **48**, 065008 (2008).
[34] F. Castejón, A. López-Fraguas, A. Tarancón, and J. L. Velasco, J. Plasma Fusion Res. **3**, S1009 (2008).
[35] M. Yokoyama, H. Maassberg, C. D. Beidler, V. Tribaldos, K. Ida, T. Estrada, F. Castejón, A. Fujisawa, T. Minami, T. Shimozuma, Y. Takeiri, A. Dinklage, S. Murakami, and H. Yamada, Nucl. Fusion **47**, 1213 (2007).
[36] J. M. Fontdecaba, F. Castejón, R. Balbín, D. López-Bruna, S. Petrov, F. Albajar, G. Cortés, J. Dies, J. García, J. Izquierdo, and J. Fontanet, Fusion Sci. Technol. **46**, 271 (2004).
[37] F. Castejón, S. Eguilior, I. Calvo, D. López-Bruna, and J. M. García-Regaña, Phys. Plasmas **15**, 012504 (2008).

[38]J. Seol, C. C. Hegna, and J. D. Callen, Phys. Plasmas **14**, 082505 (2007).
[39]R. Balbín, S. Petrov, J. M. Fontdecaba, K. J. McCarthy, V. I. Vargas, J. M. Carmona, J. Guasp, and D. Makarin, *Proceedings of the 15th International Stellarator Workshop*, Madrid, Spain, 2005 (National Institute for Fusion Science, Toki, 2005), Vol. 29C, p. D-5001.
[40]B. A. Carreras, B. Ph. van Milligen, M. A. Pedrosa, R. Balbín, C. Hidalgo, D. E. Newman, E. Sánchez, M. Frances, I. García-Cortés, J. Bleuel, M. Endler, C. Riccardi, S. Davies, G. F. Matthews, E. Martines, V. Antoni, A. Latten, and T. Klinger, Phys. Plasmas **5**, 3632 (1998).
[41]D. del-Castillo-Negrete, B. A. Carreras, and V. E. Lynch, Phys. Rev. Lett. **94**, 065003 (2005).
[42]P. Langevin, C. R. Acad. Sci. Paris **146**, 530 (1908).
[43]G. E. Uhlenbeck and L. S. Ornstein, Phys. Rev. **36**, 823 (1930).
[44]A. Fick, Ann. Phys. **170**, 59 (1855).
[45]R. Metzler and J. Klafter, Phys. Rep. **339**, 1 (2000).
[46]G. Zaslavsky, Phys. Rep. **371**, 461 (2002).
[47]I. Calvo, R. Sánchez, B. A. Carreras, and B. Ph. van Milligen, Phys. Rev. Lett. **99**, 230603 (2007).